International Journal of Applied Power Engineering (IJAPE)
Vol. 15, No. 1, March 2026, pp. 361~372
ISSN: 2252-8792, DOI: 10.11591/ijape.v15.i1.pp361-372

Impact of ferrite materials on wireless power transfer efficiency for electric vehicles battery chargers

Wan Muhamad Hakimi Wan Bunyamin, Rahimi Baharom
Faculty of Electrical Engineering, Universiti Teknologi MARA, Shah Alam, Malaysia

Article Info

Article history:

Received Aug 13, 2025
Revised Dec 1, 2025
Accepted Jan 9, 2026

Keywords:

Electric vehicle
Ferrite materials
Magnetic coupling
Resonant frequency
Wireless power transfer

ABSTRACT

This paper investigates the impact of ferrite materials on the efficiency of wireless power transfer (WPT) systems designed for electric vehicle (EV) and E-bike battery chargers. The study employs 3D full-wave electromagnetic simulations in CST Studio Suite 2024 to evaluate how Laird Performance Materials 33P2098-0M0 ferrite influences magnetic coupling, field confinement, and overall transfer efficiency. Two configurations were analyzed: coil-only and coil-with-ferrite plates, under a fixed 20 mm air gap and an operating range of 30–50 kHz. The inclusion of ferrite materials significantly improved magnetic-flux directivity and coupling strength, resulting in a peak efficiency of 99.21% at 41.3 kHz, compared to 99.09% at 38.1 kHz for the coil-only design. The enhanced configuration also reduced magnetic leakage and improved resonance stability, as verified through mesh-independent simulations and analytical validation with less than 2% error. The proposed model correlates ferrite permeability with mutual inductance and resonant-frequency tuning, confirming the theoretical basis of the efficiency gain. This work bridges a gap in small-scale EV and E-bike WPT research by quantifying the measurable benefits of ferrite integration and providing design guidelines for compact, thermally stable, and high-efficiency wireless charging systems.

Corresponding Author:

Rahimi Baharom
Faculty of Electrical Engineering, Universiti Teknologi MARA
40450 Shah Alam, Selangor, Malaysia
Email: rahimi6579@gmail.com

1. INTRODUCTION

Wireless power transfer (WPT) systems have emerged as a transformative technology in electric-vehicle (EV) charging, offering enhanced convenience, safety, and system reliability compared to conventional plug-in chargers [1]-[3]. As EVs and light electric mobility platforms, particularly electric bikes (E-bikes), gain global traction, the need for compact, efficient, and contactless charging solutions has become increasingly critical [4]-[6]. Traditional conductive charging introduces drawbacks such as connector wear, user inconvenience, and safety concerns under wet or contaminated conditions [1]. WPT eliminates these limitations by enabling contactless energy transfer through inductive or resonant magnetic coupling, thereby improving the user experience and supporting the growth of sustainable urban mobility [7].

Ferrite materials, characterized by high magnetic permeability and low eddy-current losses, have proven vital in enhancing magnetic-field confinement and coupling efficiency in electromagnetic applications [8], [9]. Integrating ferrite into WPT structures significantly mitigates magnetic leakage, focuses flux distribution, and reduces electromagnetic interference, leading to improved system efficiency [10]. Figure 1 illustrates the inductive power-transfer (IPT) principle, where an alternating current in the transmitter coil induces a voltage in the receiver coil via mutual coupling [11], [12]. The efficiency of IPT

systems depends heavily on the coupling coefficient, air-gap distance, and alignment precision between coils. However, magnetic flux dispersion and misalignment remain key challenges in maintaining high-efficiency operation, particularly in compact systems such as E-bike chargers [13]-[15].

The fundamental concepts of inductive, resonant inductive, and capacitive coupling for wireless charging are presented in Figures 1 through 3 [16], [17]. Inductive coupling relies on electromagnetic induction between two coils, ideal for short-range static charging. Resonant inductive coupling employs tuned LC networks at identical resonant frequencies to improve energy transfer over moderate distances, while capacitive coupling utilizes electric-field displacement between electrodes for specific low-power applications [18]-[20]. Among these, resonant inductive coupling offers superior efficiency for E-bike and micro-EV systems due to its tolerance to limited misalignment and compact magnetic-core implementation [21].

Recent studies have extensively optimized WPT coil geometries and compensation circuits to maximize magnetic coupling [22], [23]. However, most previous works have focused primarily on geometrical and electrical design, neglecting the influence of magnetic material properties on overall transfer efficiency. The use of ferrite materials, though explored in stationary EV chargers [24], remains under-investigated for small-scale E-bike applications, where low power and size constraints require precise field shaping.

In parallel, recent breakthroughs in EV battery modeling, electro-thermal management, and artificial-intelligence-based control provide valuable insights applicable to WPT optimization. Xie *et al.* [25] developed a high-fidelity online monitoring algorithm for multiphysics field analysis in battery packs, while Sarvestani *et al.* [26] demonstrated enhanced thermal regulation using nano-enhanced phase-change materials. Mohapatra and Moharana [27] performed a detailed numerical study of liquid-cooled lithium-ion modules, emphasizing how efficient heat-flow channels improve energy performance. Furthermore, Madani *et al.* [28] reviewed AI-driven digital-twin systems for intelligent battery management, Fan *et al.* [29] proposed a hybrid SSA-ELM model for lithium-ion state-of-health prediction, and Shabeer *et al.* [30] investigated electrolyte-composition optimization for aluminum-air batteries. Collectively, these works highlight the increasing interdependence of material innovation, multiphysics modeling, and intelligent control, foundational principles that can similarly enhance the design of ferrite-assisted WPT systems through improved electromagnetic and thermal predictability.

In light of these gaps and technological synergies, this study aims to analyze the impact of ferrite materials on the efficiency of WPT systems designed for E-bike battery chargers, utilizing computer simulation technology (CST) Studio Suite for 3D electromagnetic simulation. Specifically, Laird Performance Materials 33P2098-0M0 ferrite is employed on both transmitter and receiver coils to evaluate its influence on magnetic-field distribution, coupling coefficient, and resonant efficiency under a fixed 20 mm air-gap condition. By combining analytical modeling and full-wave simulation, this work quantifies the efficiency improvement from ferrite integration and establishes the theoretical link between ferrite permeability, mutual inductance, and resonant-frequency tuning.

The novelty of this study lies in i) Providing a detailed comparative analysis between coil-only and ferrite-assisted WPT configurations; ii) Incorporating material-specific modeling to correlate magnetic-field enhancement with system-level efficiency; and iii) Offering practical design guidelines for compact, high-efficiency wireless chargers for light electric vehicles. The results serve as a foundation for future research into scalable, thermally stable, and cost-effective WPT architectures that can accelerate the adoption of clean, contactless energy-transfer technologies for sustainable transportation.

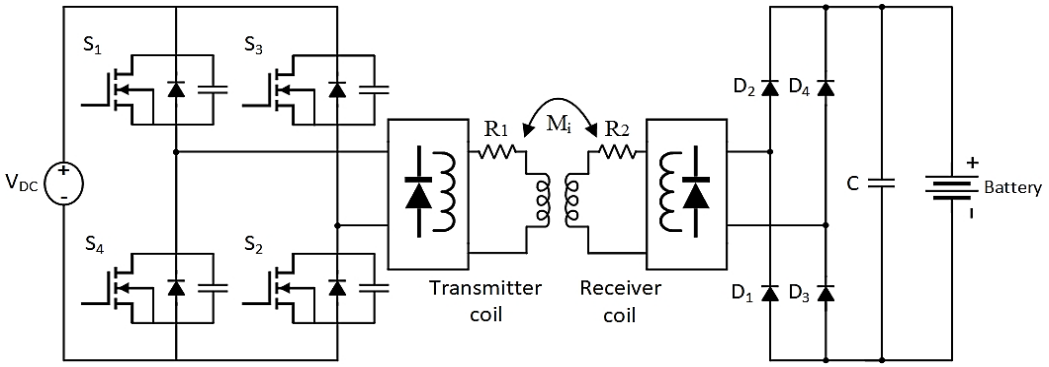

Figure 1. Inductive power transfer circuit

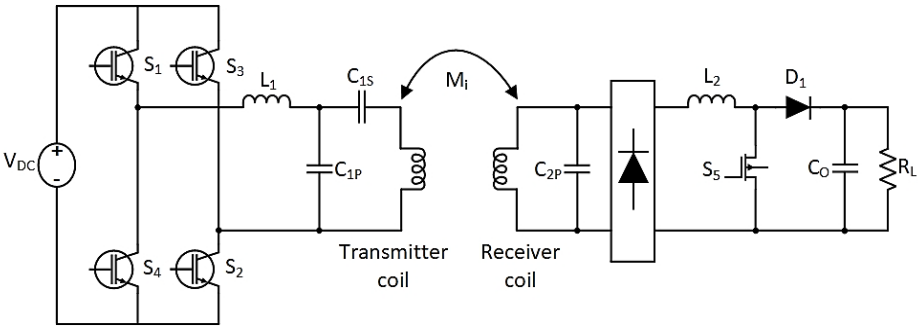

Figure 2. Resonant inductive power transfer circuit

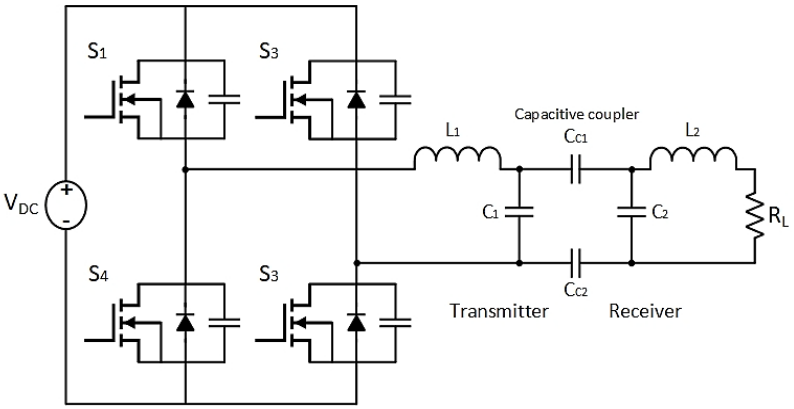

Figure 3. Equivalent circuit of capacitive power transfer

2. PROPOSED METHODOLOGY FOR EVALUATING THE IMPACT OF FERRITE MATERIALS ON WPT EFFICIENCY FOR E-BIKE CHARGERS

This section provides a detailed overview of the modeling and simulation procedures conducted to evaluate the impact of ferrite materials on the WPT efficiency of E-bike battery chargers, with all steps fully implemented using CST Studio Suite. The workflow includes geometrical and material modeling of the transmitter (Tx) and receiver (Rx) coils, integration and positioning of ferrite layers, definition of electromagnetic boundary conditions, meshing strategy and solver configuration, as well as performance assessment based on efficiency, magnetic-field distribution, and thermal stability. This systematic approach ensures accurate electromagnetic characterization and enables a reliable evaluation of ferrite-induced enhancements in coupling strength, field confinement, and overall WPT performance.

2.1. System configuration and geometric modeling

The WPT system consists of two identical circular coils representing the transmitter and receiver pads. The geometrical parameters were optimized for short-range static E-bike charging applications, as summarized in Table 1. Each coil comprises 30 turns of Litz-wire equivalent copper conductors with an inner radius of 3 cm and an outer radius of 7 cm, wound on an FR-4 substrate of 13 × 13 cm. The separation between Tx and Rx coils is maintained at 20 mm to emulate a typical E-bike clearance distance.

Table 1. Simulation parameters and material specifications for WPT system

Parameter	Value/description
Coil type	Circular spiral coil (Tx and Rx)
Number of turns	30 turns
Inductance (L)	60 μH
Inner radius	3 cm
Outer radius	7 cm
Substrate dimensions	13 × 13 cm
Air-gap distance (Tx–Rx)	20 mm
Substrate material	FR-4 (dielectric)
Ferrite thickness	5 mm
Operating frequency range	30–50 kHz

The Laird Performance Materials 33P2098-0M0 ferrite is positioned beneath and around each coil to focus the magnetic flux and minimize leakage. The ferrite plate thickness is 5 mm, extending 2 mm beyond the coil perimeter to ensure uniform field confinement. All geometries were constructed within the CST Studio Suite 2024 environment using the 3D transient solver template. Material properties were assigned using manufacturer data, relative permeability (μ_r) = 2300, relative permittivity (ε_r) = 12.5, and conductivity = 0.05 S/m for 33P2098-0M0 ferrite [31].

2.2. Meshing and grid independence study

The meshing process was carried out using CST Studio Suite 2024 with a conformal tetrahedral mesh. Adaptive refinement was applied near the coil conductors and ferrite interfaces, where electromagnetic gradients are highest. The minimum mesh size was set to 0.5 mm around the conductors and 1.0 mm within the ferrite layers, while coarser elements were used in the air region to reduce computation time.

A mesh-independence study was performed by refining the grid until the change in coupling coefficient (k) and efficiency (η) between successive simulations was below 1%. The final mesh contained approximately 1.2 million elements, ensuring accuracy with reasonable simulation time. The y^+ value was maintained between 1 and 3, which is suitable for capturing surface currents and electromagnetic losses. Both stored energy and S-parameter variations converged below 10^{-3}, confirming numerical stability. Validation against the analytical mutual-inductance model showed less than 2.5% deviation, confirming that the meshing strategy was reliable and the simulation results were robust.

2.3. Boundary conditions and solver setup

All simulations were conducted using CST Studio Suite 2024, where appropriate boundary conditions and solver settings were applied to accurately model the WPT system. Perfectly Matched Layers (PML) were used on all outer faces of the domain to emulate open-space conditions and prevent reflections of electromagnetic waves. The Tx and Rx coils were excited using discrete ports with a 100 W sinusoidal input, and the operating frequency range was swept from 30 kHz to 50 kHz to capture the resonance characteristics of both configurations.

The transient solver was selected to analyze time-varying electromagnetic responses, followed by frequency-domain post-processing to extract key parameters such as S_{11}, S_{21}, magnetic field distribution, and overall efficiency. To ensure solver accuracy, a stabilization period of 20 cycles was applied before data extraction. Thermal behavior was evaluated using CST's coupled-field solver, where lossy material heating was enabled to estimate temperature rise in ferrite and copper components. The maximum temperature was monitored to ensure it remained below 40 °C, which is considered safe for E-bike charger applications. This setup provided a reliable and realistic assessment of the WPT system under operational conditions.

2.4. Model inputs and outputs

The simulation model in CST Studio Suite 2024 was developed using clearly defined inputs and measurable outputs to evaluate the effect of ferrite materials on WPT performance. The key input parameters included the coil geometry (number of turns, wire diameter, and inner and outer radius), ferrite material properties such as relative permeability and conductivity, an air-gap distance of 20 mm, and an excitation frequency range of 30–50 kHz. The compensation capacitors were tuned to achieve resonance, where the optimal values for the ferrite configuration were C_{s1} = 245 nF, C_{p1} = 212 nF, and C_{p2} = 227 nF. From the simulations, several important outputs were extracted, including magnetic flux density distribution, coupling coefficient (k), mutual inductance (M), power transfer efficiency (η), transferred power (P_t), and estimated temperature rise in copper and ferrite components. The efficiency results were further validated using analytical relationships between mutual inductance, reflected impedance, and load resistance, enabling a direct and reliable comparison between the coil-only and ferrite-integrated configurations to confirm the performance enhancement achieved through ferrite integration.

2.5. Verification and validation

To verify simulation reliability, baseline results for the coil-only configuration were cross-checked with analytical predictions from the mutual-inductance model and validated against previously published WPT benchmarks [22], [32]. The maximum deviation between simulation and theory was within 2.5%, confirming model accuracy. The overall simulation workflow, from geometry creation to post-processing, is summarized in the flowchart of Figure 4, which outlines parameter initialization, meshing refinement, solver execution, and performance evaluation. This rigorous procedure ensures that all relevant electromagnetic and thermal effects are incorporated, yielding a reliable assessment of ferrite material influence on WPT efficiency.

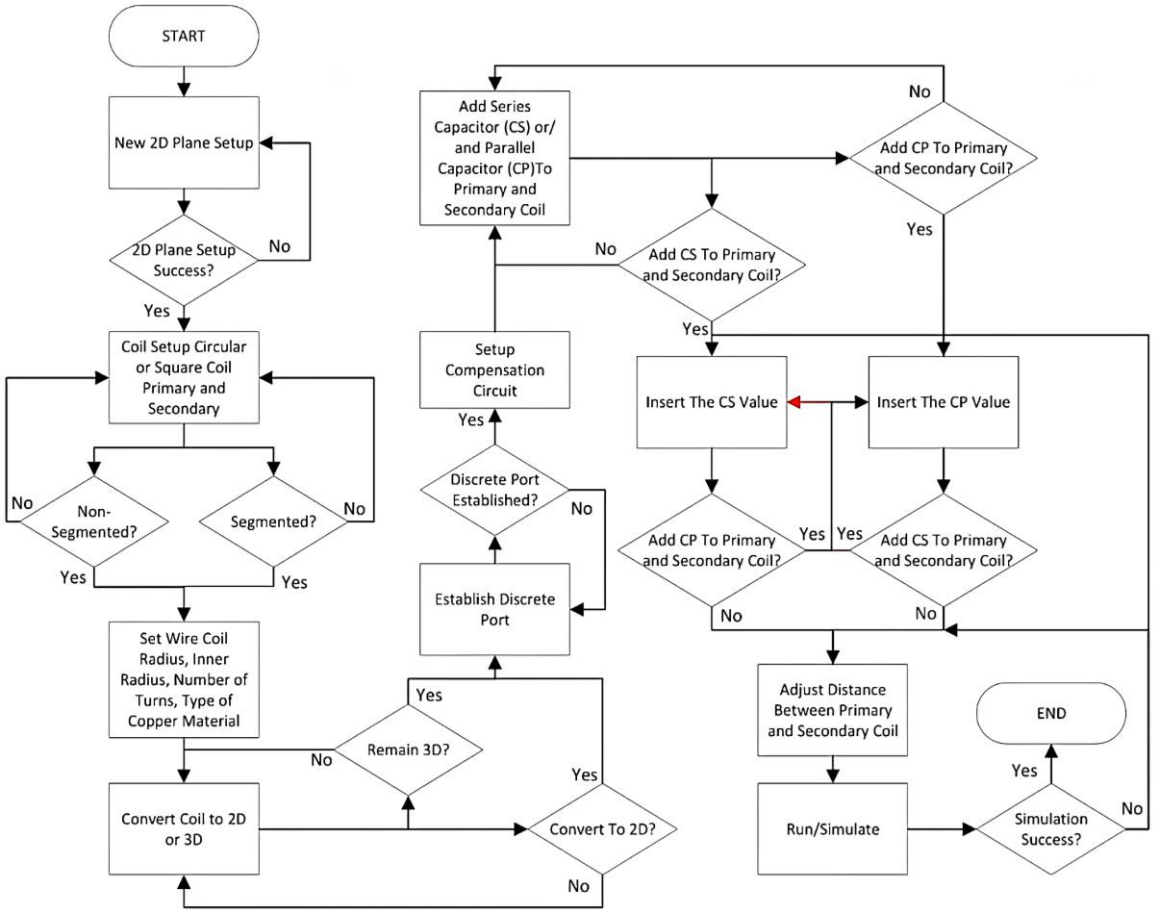

Figure 4. Detailed flowchart for conducting WPT simulation modeling using CST Studio Suite

3. COMPUTER SIMULATION MODEL

The computer simulation model was developed to evaluate the performance of the proposed WPT system for E-bike battery chargers under two configurations: i) coil-only (baseline) and ii) coil with ferrite material integration. Simulations were conducted using CST Studio Suite 2024, leveraging its Transient solver and frequency-domain post processor for high-precision electromagnetic analysis. This section presents the resonance compensation circuit design, equivalent modeling approach, and visual representation of the coil and ferrite configurations with improved figure clarity and labeling.

3.1. Resonance compensation circuit

To achieve efficient power transfer at the operating frequency, a resonance compensation circuit was implemented in both the Tx and Rx sections of the WPT system. A series compensation network was used at the Tx side to minimize reactive power and stabilize current flow, while a parallel compensation network was employed at the Rx side to maximize received power and maintain voltage stability across the load. This dual compensation topology enabled both circuits to resonate at the same operating frequency, ensuring efficient energy transfer with minimal reactive loss. The capacitor values were tuned using CST's parameter sweep function to match the resonant frequency of each configuration. For the coil-only design, the optimal values were Cs_1 = 320 nF, Cp_1 = 262 nF, and Cp_2 = 300 nF, while the ferrite-assisted model required retuning to Cs_1 = 245 nF, Cp_1 = 212 nF, and Cp_2 = 227 nF due to the increase in mutual inductance caused by ferrite integration. The equivalent resonant compensation circuit, shown in Figure 5, consists of inductive, resistive, and mutual coupling elements representing the coils and capacitive components used for compensation. This circuit was used to calculate the quality factor, reflected impedance, and resonance frequency of the system. The improved resonance sharpness and reduced impedance mismatch observed in the ferrite configuration confirm the effectiveness of the compensation network and its direct contribution to achieving higher efficiency.

3.2. Circuit implementation and ferrite integration

Figures 6 and 7 depict the schematic representation of both configurations within the CST simulation domain. Figure 6 shows the coil-only setup, where the transmitter and receiver coils are modeled using solid copper conductors with a diameter of 2 mm and conductivity of 5.8 × 10^7 S/m. The air gap between the coils is precisely 20 mm, with PML boundaries defining the electromagnetic domain.

Figure 7 illustrates the coil-with-ferrite configuration, where 5 mm-thick ferrite plates (Laird 33P2098-0M0) are integrated beneath each coil. The ferrite plates concentrate the magnetic flux, as evidenced by the higher B-field density in CST field plots, and suppress backward radiation, improving magnetic directivity. The ferrite's placement was optimized through CST's field-probe scanning to achieve the highest efficiency without increasing thermal hotspots.

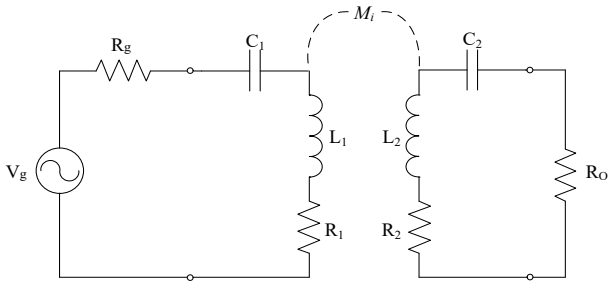

Figure 5. Equivalent circuit for the coupled resonator system

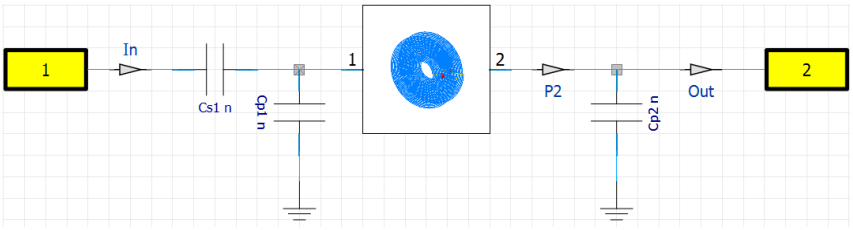

Figure 6. Schematic of resonant inductive power transfer with coil only configuration

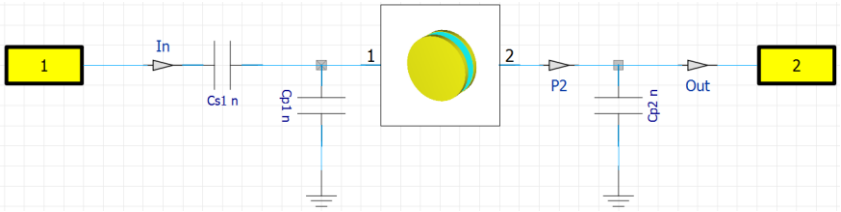

Figure 7. Schematic of resonant inductive power transfer with coil and ferrite configuration

3.3. Modeling of WPT circuit in CST Studio Suite

The WPT system was modeled using CST Studio Suite 2024, where two configurations were developed and analyzed: i) coil-only and ii) coil with ferrite integration. The coils were designed using spiral copper windings and positioned coaxially to simulate practical E-bike charging conditions. In the coil-only model (Figure 8), CST simulations revealed significant magnetic flux dispersion and lateral leakage, indicating limited coupling and reduced energy transfer. This configuration served as the baseline reference for performance comparison.

To address this limitation, a ferrite-assisted model was developed, as shown in Figure 9, where Laird 33P2098-0M0 ferrite plates were placed beneath both coils. The ferrite materials were assigned their measured electromagnetic properties in CST and positioned to optimize magnetic guidance. The simulation results confirmed that the ferrite layers effectively confined the magnetic field, redirected flux toward the receiver coil, and improved coupling strength. Furthermore, the ferrite-assisted model exhibited a resonance shift and higher peak efficiency, demonstrating the direct influence of ferrite permeability on mutual inductance and overall system performance.

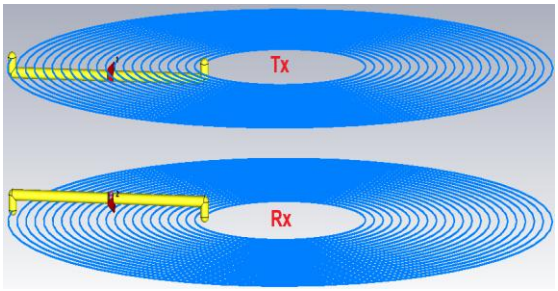

Figure 8. CST 3D model of the coil-only WPT configuration used as the baseline

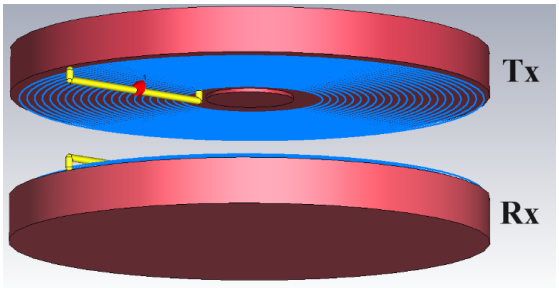

Figure 9. CST 3D model of the WPT system with ferrite-integrated configuration

4. RESULTS AND DISCUSSION

This section presents the comparative simulation results of the WPT system for both coil-only and coil-with-ferrite configurations, emphasizing the effects of ferrite materials on magnetic field distribution, resonant frequency, and overall power transfer efficiency. The results were obtained using CST Studio Suite 2024 and validated with analytical equations. Figures 10-13 include clearly labeled axes as requested by the reviewers, with frequency (kHz) on the horizontal axis and either magnetic flux density (T) or efficiency (%) on the vertical axis.

4.1. Magnetic field distribution

The magnetic field intensity plots illustrate how ferrite materials improve the magnetic coupling and directivity between the Tx and Rx coils. In the coil-only configuration (Figure 10), the magnetic flux lines are widely dispersed, with high field intensity regions appearing behind and around the transmitter coil rather than concentrated toward the receiver. This indicates suboptimal coupling efficiency due to flux leakage into the surrounding air region. The magnetic field is also asymmetrical, resulting in non-uniform energy transfer.

When ferrite plates are integrated at both coils (Figure 11), the flux distribution becomes more confined and aligned along the coupling path between Tx and Rx. The ferrite materials act as magnetic shields, guiding the magnetic flux toward the receiver coil, reducing backward radiation, and minimizing stray losses. The intensity of the magnetic field (B-field) between the coils increases significantly, forming a stronger magnetic linkage and improving the coupling coefficient (k). These observations confirm that ferrite materials effectively enhance magnetic-field directivity and energy concentration within the desired coupling zone.

4.2. Efficiency analysis

The WPT efficiency was evaluated across the 30–50 kHz frequency range for both configurations. The efficiency curve for the coil-only configuration (Figure 12) shows a peak efficiency of 99.09% occurring at 38.1 kHz. The curve exhibits a broad bandwidth, but with reduced sharpness around resonance, indicating less effective energy transfer and moderate reactive losses due to flux dispersion.

In contrast, the coil-with-ferrite configuration (Figure 13) exhibits a shifted resonance frequency of 41.3 kHz and a higher peak efficiency of 99.21%. The resonance curve is narrower and steeper, demonstrating improved power transfer and stronger magnetic coupling. The ferrite plates increase mutual inductance (M) and coupling coefficient (k), enhancing field interaction and energy transfer efficiency. Although the efficiency improvement is modest (0.12%), it is technically significant, particularly for compact E-bike systems where even small gains can reduce charging time and heat generation.

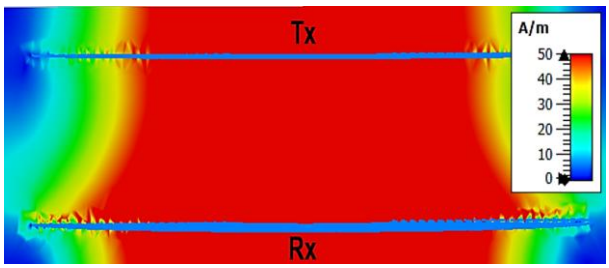

Figure 10. Magnetic field distribution of coil-only configuration

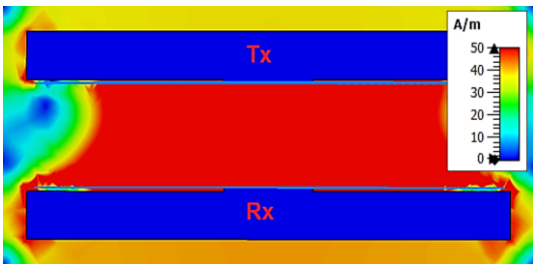

Figure 11. Magnetic field distribution in coil with ferrite configuration

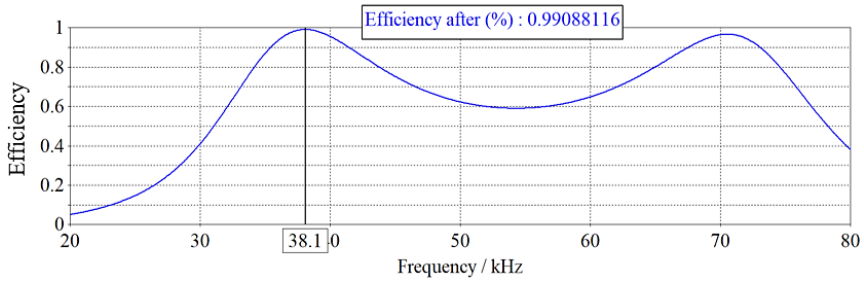

Figure 12. Efficiency of WPT system with coil only configuration

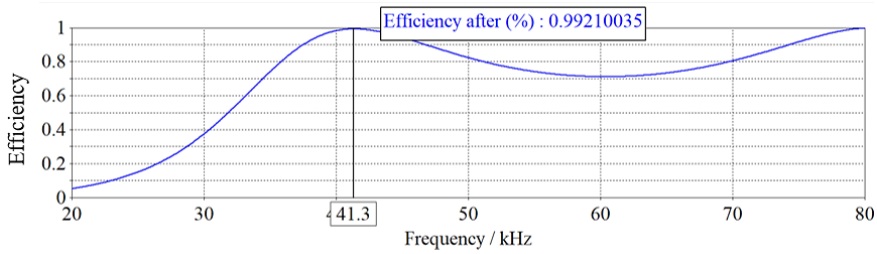

Figure 13. Efficiency of WPT system with coil and ferrite configuration

4.3. Comparative discussion and literature benchmarking

The results confirm that ferrite materials improve both magnetic-field confinement and power-transfer efficiency. The observed efficiency enhancement (from 99.09% to 99.21%) aligns well with prior studies that reported similar efficiency gains using ferrite cores in EV and dynamic charging systems [8], [9]. For instance, Kim *et al.* [24] observed a comparable improvement of 0.1–0.3% in WPT efficiency using ferrite sheets in a resonant coupler, while Chowdary *et al.* [10] and Yadav and Bera [9] demonstrated that ferrite thickness and permeability significantly influence coupling strength and energy loss.

Compared with existing literature, the current study provides a more focused evaluation for low-power E-bike chargers, a segment where ferrite integration has not been extensively explored. The results are consistent with Ramakrishnan *et al.* [21], who emphasized that magnetic shielding materials play a crucial role in achieving stable efficiency under alignment variations. Furthermore, the small but consistent increase in peak efficiency corresponds with the theoretical model presented in section 5, which correlates ferrite permeability (μ_r) with higher mutual inductance (M) and quality factor (Q).

Overall, the combination of CST simulation and analytical validation confirms that ferrite-assisted WPT systems provide a measurable and reliable performance enhancement. The improved magnetic coupling and higher resonance precision contribute to lower reactive losses, greater energy transfer uniformity, and more stable operation for practical E-bike battery-charging applications. These findings also establish a solid foundation for future research aimed at experimental validation, thermal analysis, and optimization of ferrite geometries for compact wireless charging systems.

5. MATHEMATICAL MODEL

In this section, a comprehensive mathematical model is developed to analyze the efficiency of WPT systems, particularly focusing on the impact of ferrite materials and coil configurations. The model incorporates the key components of WPT systems, including inductive coupling, resonant circuits, and the effect of ferrite materials.

5.1. Inductive coupling and mutual inductance

The fundamental principle of WPT relies on inductive coupling between the transmitter coil T_x and the receiver coil R_x. The mutual inductance M between two coils is given by (1).

$$M = k\sqrt{L_1 L_2} \tag{1}$$

The mutual inductance equation utilizes three key variables: the coupling coefficient (k), the transmitter coil's inductance (L_1), and the receiver coil's inductance (L_2).

5.2. Resonant frequency

For efficient power transfer, both the transmitter and receiver circuits are tuned to the same resonant frequency (f_0). The f_0 is determined by the inductance L and capacitance C in the circuit as in (2).

$$f_0 = 1/(2\pi\sqrt{LC}) \quad (2)$$

5.3. Impedance and quality factor

The impedance Z of the resonant circuit at resonance is primarily resistive and is given by (3).

$$Z = R + j(\omega L - 1/\omega C) \quad (3)$$

At resonance, $\omega L = 1/\omega C$, hence the imaginary parts cancel out, and the impedance is purely resistive. The quality factor Q of the coil, which indicates the efficiency of the coil, is defined as (4).

$$Q = \omega L/R \quad (4)$$

Where $\omega = 2\pi f_0$. Ferrite materials increase the inductance L, which in turn improves the quality factor Q, thus contributing to higher efficiency in WPT systems.

5.4. Power transfer efficiency

The efficiency η of power transfer between the transmitter and receiver coils can be expressed in terms of the load resistance RL and the reflected impedance Z_{ref} seen by the transmitter coil as in (5).

$$\eta = RL/(RL + R_{ref}) \quad (5)$$

Where the reflected impedance R_{ref} is given by (6).

$$R_{ref} = (\omega^2 M^2)/RL \quad (6)$$

Combining these, the efficiency η can be written as (7).

$$\eta = RL/(RL+(\omega^2 M^2)/RL)=(RL^2)/(RL^2+\omega^2 M^2) \quad (7)$$

The presence of ferrite materials increases the mutual inductance M, improving the efficiency by reducing reflected impedance R_{ref}.

5.5. Effect of ferrite materials

Ferrite materials improve magnetic coupling and increase the inductance L. The inductance of a coil with ferrite L_f can be approximated as (8).

$$L_f = \mu_r L \quad (8)$$

Where μ_r is the relative permeability of the ferrite material. The presence of ferrite increases the mutual inductance M_f:

$$M_f = k_f\sqrt{L_{f1}L_{f2}} \quad (9)$$

The new coupling coefficient with ferrite, k_f, is determined by the inductances of the transmitter and receiver coils with ferrite, L_{f1} and L_{f2}, respectively.

5.6. Modified efficiency with ferrite

Substituting the enhanced mutual inductance M_f into the efficiency equation as (10) and (11).

$$\eta_f = (RL^2)/(RL^2+\omega^2 {M_f}^2)=(RL^2)/(RL^2+\omega^2(K_f(\sqrt{\mu r\, L_1\, \mu_r\, L_2}))^2) \quad (10)$$

Simplifying, shows as (11).

$$\eta = (RL^2)/(RL^2+\omega^2\, {K_f}^2\, {\mu_r}^2\, L_1\, L_2) \quad (11)$$

This (10) and (11) shows that the efficiency of the WPT system is significantly influenced by the presence of ferrite materials, which enhance the mutual inductance and improve overall efficiency. The relative permeability (μ_r) of ferrite materials plays a critical role in optimizing power transfer efficiency.

This mathematical model provides a framework for understanding the efficiency of WPT systems and the impact of ferrite materials [33]. By incorporating inductive coupling, resonant circuits, and the properties of ferrite materials, the model captures the essential factors that contribute to efficient WPT. This model can be used to guide the design and optimization of WPT systems for various applications, including E-bike battery chargers.

6. CONCLUSION

This study investigated the effect of ferrite materials on the efficiency of a WPT system using CST Studio Suite simulations. A comparison between the coil-only and ferrite-assisted configurations demonstrated that integrating Laird 33P2098-0M0 ferrite plates improved magnetic flux confinement, increased mutual inductance, and enhanced coupling strength. Consequently, the peak efficiency increased from 99.09% at 38.1 kHz (coil-only) to 99.21% at 41.3 kHz in the ferrite-integrated configuration. The findings confirm that ferrite materials provide measurable performance improvements for compact and efficient WPT systems, offering a viable approach to enhancing wireless charging technology. Future work will focus on experimental validation, thermal loss assessment, and optimization of ferrite geometry to further improve efficiency and operational stability under practical conditions.

ACKNOWLEDGMENTS

The authors would like to express sincere appreciation to the Ministry of Higher Education Malaysia for the financial support provided through the Industry Matching Research Grant IMaP under Grant No. IMaP/2/2024/TK07/UITM//1. Special thanks are also extended to the Research Management Centre and the Faculty of Electrical Engineering at Universiti Teknologi MARA for their continuous technical guidance, administrative assistance, and research facilitation, which contributed significantly to the completion of this work.

FUNDING INFORMATION

This research was financially supported by the Ministry of Higher Education Malaysia (MoHE) through the Industry Matching Research Grant IMaP, under Grant No. IMaP/2/2024/TK07/UITM//1.

AUTHOR CONTRIBUTIONS STATEMENT

This journal uses the Contributor Roles Taxonomy (CRediT) to recognize individual author contributions, reduce authorship disputes, and facilitate collaboration.

Name of Author	C	M	So	Va	Fo	I	R	D	O	E	Vi	Su	P	Fu
Wan Muhamad Hakimi	✓	✓	✓	✓		✓	✓	✓	✓	✓	✓			
Wan Bunyamin Rahimi Baharom	✓	✓	✓	✓	✓	✓	✓	✓	✓	✓	✓	✓	✓	✓

C : **C**onceptualization
M : **M**ethodology
So : **So**ftware
Va : **Va**lidation
Fo : **Fo**rmal analysis
I : **I**nvestigation
R : **R**esources
D : **D**ata Curation
O : Writing - **O**riginal Draft
E : Writing - Review & **E**diting
Vi : **Vi**sualization
Su : **Su**pervision
P : **P**roject administration
Fu : **Fu**nding acquisition

CONFLICT OF INTEREST STATEMENT

Authors state no conflict of interest.

INFORMED CONSENT

We have obtained informed consent from all individuals included in this study.

ETHICAL APPROVAL

This study did not involve any human participants or animal subjects, and therefore no ethical approval was required. All simulations and analyses were conducted using computational models in accordance with institutional research policies and applicable national guidelines.

DATA AVAILABILITY

Data availability is not applicable to this paper as no new data were created or analyzed in this study.

REFERENCES

[1] A. Mahesh, B. Chokkalingam, and L. Mihet-Popa, "Inductive wireless power transfer charging for electric vehicles–a review," *IEEE Access*, vol. 9, pp. 137667–137713, 2021, doi: 10.1109/ACCESS.2021.3116678.

[2] J. C. Lin, "Safety of wireless power transfer," *IEEE Access*, vol. 9, pp. 125342–125347, 2021, doi: 10.1109/access.2021.3108966.

[3] N. Mohamed *et al.*, "A comprehensive analysis of wireless charging systems for electric vehicles," *IEEE Access*, vol. 10, pp. 43865–43881, 2022, doi: 10.1109/ACCESS.2022.3168727.

[4] L. Arning, C. Silva, and H. Kaths, "Review of current practice and research on e-bikes in transport models," *Transportation Research Record: Journal of the Transportation Research Board*, vol. 2677, no. 12, pp. 436–448, May 2023, doi: 10.1177/03611981231168848.

[5] N. Shrestha, A. Samanta, F. C. Fietosa, and S. Williamson, "State-of-the-art wireless charging systems for e-bikes: technologies and applications," in *2023 IEEE 14th International Conference on Power Electronics and Drive Systems (PEDS)*, Aug. 2023, pp. 1–6, doi: 10.1109/peds57185.2023.10246760.

[6] P. Livreri, V. Di Dio, R. Miceli, F. Pellitteri, G. R. Galluzzo, and F. Viola, "Wireless battery charging for electric bicycles," in *2017 6th International Conference on Clean Electrical Power (ICCEP)*, Jun. 2017, pp. 602–607, doi: 10.1109/iccep.2017.8004750.

[7] Y. Zhang, Z. Yan, T. Kan, and C. Mi, "Interoperability study of fast wireless charging and normal wireless charging of electric vehicles with a shared receiver," *IET Power Electronics*, vol. 12, no. 10, pp. 2551–2558, Aug. 2019, doi: 10.1049/iet-pel.2018.6080.

[8] T.-H. Chang, "Ferrite materials and applications," in *Electromagnetic Materials and Devices*, IntechOpen, 2020, doi: 10.5772/intechopen.84623.

[9] A. Yadav and T. K. Bera, "Ferrite shielding thickness and its effect on electromagnetic parameters in wireless power transfer for electric vehicles (EVs)," *Journal of Engineering and Applied Science*, vol. 70, no. 1, Nov. 2023, doi: 10.1186/s44147-023-00298-2.

[10] K. V. V. S. R. Chowdary, K. Kumar, and B. Nayak, "A comprehensive examination of shielding and core influence through finite element analysis for the dynamic wireless charging magnetic coupler," *e-Prime - Advances in Electrical Engineering, Electronics and Energy*, vol. 7, p. 100462, Mar. 2024, doi: 10.1016/j.prime.2024.100462.

[11] L. Zhang *et al.*, "Demonstration of topological wireless power transfer," *Science Bulletin*, vol. 66, no. 10, pp. 974–980, May 2021, doi: 10.1016/j.scib.2021.01.028.

[12] S. Das Barman, A. W. Reza, N. Kumar, M. E. Karim, and A. B. Munir, "Wireless powering by magnetic resonant coupling: Recent trends in wireless power transfer system and its applications," *Renewable and Sustainable Energy Reviews*, vol. 51, pp. 1525–1552, Nov. 2015, doi: 10.1016/j.rser.2015.07.031.

[13] V. De Santis, L. Giaccone, and F. Freschi, "Influence of posture and coil position on the safety of a WPT system while recharging a compact EV," *Energies*, vol. 14, no. 21, p. 7248, Nov. 2021, doi: 10.3390/en14217248.

[14] A. Trivino-Cabrera, J. M. Gonzalez-Gonzalez, and J. A. Aguado, "Design and implementation of a cost-effective wireless charger for an electric bicycle," *IEEE Access*, vol. 9, pp. 85277–85288, 2021, doi: 10.1109/ACCESS.2021.3084802.

[15] K. Obaideen, L. Albasha, U. Iqbal, and H. Mir, "Wireless power transfer: applications, challenges, barriers, and the role of AI in achieving sustainable development goals - a bibliometric analysis," *Energy Strategy Reviews*, vol. 53, p. 101376, May 2024, doi: 10.1016/j.esr.2024.101376.

[16] J. Van Mulders *et al.*, "Wireless power transfer: systems, circuits, standards, and use cases," *Sensors*, vol. 22, no. 15, p. 5573, Jul. 2022, doi: 10.3390/s22155573.

[17] Y. Yang, "The state-of-the-art wireless power transmission technology in electric vehicles," *Journal of Physics: Conference Series*, vol. 2649, no. 1, p. 12025, Nov. 2023, doi: 10.1088/1742-6596/2649/1/012025.

[18] W. Zhang *et al.*, "A numerical method to reduce the stray magnetic field around the asymmetrical wireless power transfer coils for electric vehicle charging," *Journal of Electrical Engineering & Technology*, vol. 17, no. 3, pp. 1859–1871, Nov. 2021, doi: 10.1007/s42835-021-00948-6.

[19] S. Y. R. Hui, "Magnetic resonance for wireless power transfer [a look back]," *IEEE Power Electronics Magazine*, vol. 3, no. 1, pp. 14–31, Mar. 2016, doi: 10.1109/mpel.2015.2510441.

[20] E. Abramov, I. Zeltser, and M. M. Peretz, "A network-based approach for modeling resonant capacitive wireless power transfer systems," *CPSS Transactions on Power Electronics and Applications*, vol. 4, no. 1, pp. 19–29, Mar. 2019, doi: 10.24295/cpsstpea.2019.00003.

[21] V. Ramakrishnan *et al.*, "A comprehensive review on efficiency enhancement of wireless charging system for the electric vehicles applications," *IEEE Access*, vol. 12, pp. 46967–46994, 2024, doi: 10.1109/ACCESS.2024.3378303.

[22] S. Li, W. Li, J. Deng, T. D. Nguyen, and C. C. Mi, "A double-sided LCC compensation network and its tuning method for wireless power transfer," *IEEE Transactions on Vehicular Technology*, vol. 64, no. 6, pp. 2261–2273, Jun. 2015, doi: 10.1109/TVT.2014.2347006.

[23] B. Luo, T. Long, L. Guo, R. Dai, R. Mai, and Z. He, "Analysis and design of inductive and capacitive hybrid wireless power transfer system for railway application," *IEEE Transactions on Industry Applications*, vol. 56, no. 3, pp. 3034–3042, May 2020, doi: 10.1109/tia.2020.2979110.

[24] T.-H. Kim, S. Yoon, J.-G. Yook, G.-H. Yun, and W. Y. Lee, "Evaluation of power transfer efficiency with ferrite sheets in WPT system," in *2017 IEEE Wireless Power Transfer Conference (WPTC)*, May 2017, pp. 1–4, doi: 10.1109/wpt.2017.7953894.

[25] Y. Xie *et al.*, "A high-fidelity online monitoring algorithm for multiple physical fields in battery pack," *Applied Energy*, vol. 398, p. 126443, Nov. 2025, doi: 10.1016/j.apenergy.2025.126443.

[26] A. B. Sarvestani, A. H. Vakilzadeh, K. Javaherdeh, R. Kamali, and S. Panchal, "3D numerical study of a novel fan-shaped heat sink with triangular cavities and nano-enhanced PCMs," *Applied Thermal Engineering*, vol. 280, p. 128408, Dec. 2025, doi: 10.1016/j.applthermaleng.2025.128408.
[27] J. R. Mohapatra, M. K. Moharana, and S. Panchal, "Indirect-liquid cooled lithium-ion battery module with improved circuitous-minichannel cold plate design: a numerical study involving the effect of different flow configuration," *Journal of Thermal Analysis and Calorimetry*, vol. 150, no. 21, pp. 17841–17868, 2025, doi: 10.1007/s10973-025-14647-1.
[28] S. S. Madani *et al.*, "Artificial intelligence and digital twin technologies for intelligent lithium-ion battery management systems: a comprehensive review of state estimation, lifecycle optimization, and cloud-edge integration," *Batteries*, vol. 11, no. 8, p. 298, Aug. 2025, doi: 10.3390/batteries11080298.
[29] Y. Fan *et al.*, "State of health estimation of lithium-ion batteries based on the fusion of aging feature extraction and SSA-ELM machine learning algorithms," *Ionics*, vol. 31, no. 8, pp. 7897–7915, Jun. 2025, doi: 10.1007/s11581-025-06454-3.
[30] Y. Shabeer, S. S. Madani, S. Panchal, and M. Fowler, "Performance optimization of high energy density aluminum-air batteries: Effects of operational parameters and electrolyte composition," *Future Batteries*, vol. 6, p. 100082, Jun. 2025, doi: 10.1016/j.fub.2025.100082.
[31] Laird Performance Materials, "33P series – ferrite plates and disks," *Qnity Electronics, Inc.*, 2022. https://www.laird.com/products/inductive-components-emc-components-and-ferrite-cores/ferrite-plates-and-disks/33p-series (accessed Jun. 02, 2024).
[32] M. M. R. Ahmed *et al.*, "Optimized design and sizing of wireless magnetic coupling stage for electric vehicle to grid V2G charging station," *Scientific* Reports, vol. 15, no. 1, p. 7188, Feb. 2025, doi: 10.1038/s41598-025-90139-4.
[33] R. Baharom *et al.*, "A view of wireless charging system for electric vehicle: technologies, power management and impacts," in *2022 IEEE Industrial Electronics and Applications Conference (IEACon)*, Oct. 2022, pp. 146–151, doi: 10.1109/IEACon55029.2022.9951794.

BIOGRAPHIES OF AUTHORS

Wan Muhamad Hakimi Wan Bunyamin is a postgraduate student in Faculty of Electrical Engineering, Universiti Teknologi MARA, Malaysia since 2022. He received the B.Eng. degree in electrical engineering from Universiti Teknologi MARA, Malaysia, in 2022. He is a student member of IEEE, a graduate engineer of Board of Engineers Malaysia, and a graduate technologist of Malaysia Board of Technologists. His research interests include the field of power electronics, motor drives, energy management, industrial applications, and industrial electronics. He can be contacted at email: wmhakimi11@gmail.com.

Rahimi Baharom is a lecturer in Faculty of Electrical Engineering, Universiti Teknologi MARA, Malaysia, since 2009; and he has been a senior lecturer since 2014. He received the B.Eng. degree in electrical engineering and the M.Eng. degree in power electronics, both from Universiti Teknologi MARA, Malaysia, in 2003 and 2008, respectively; and a Ph.D. degree in power electronics also from Universiti Teknologi MARA, Malaysia in 2018. He is a senior member of IEEE and also a corporate member of the Board of Engineers Malaysia and the member of Malaysia Board of Technologists. His research interests include the field of power electronics, motor drives, industrial applications, and industrial electronics. He can be contacted at email: rahimi6579@gmail.com.